blood®
Regular Article

LYMPHOID NEOPLASIA

Whole-genome CRISPR screening identifies molecular mechanisms of PD-L1 expression in adult T-cell leukemia/lymphoma

Masahiro Chiba,[1,*] Joji Shimono,[1,*] Keito Suto,[1] Takashi Ishio,[1] Tomoyuki Endo,[1] Hideki Goto,[1] Hiroo Hasegawa,[2] Michiyuki Maeda,[3] Takanori Teshima,[1] Yibin Yang,[4] and Masao Nakagawa[1]

[1]Department of Hematology, Hokkaido University Faculty of Medicine, Sapporo, Japan; [2]Department of Laboratory Medicine, Nagasaki University Hospital, Nagasaki, Japan; [3]Institute for Frontier Life and Medical Sciences, Kyoto University, Kyoto, Japan; and [4]Blood Cell Development and Function Program, Fox Chase Cancer Center, Philadelphia, PA

KEY POINTS

- **Whole-genome CRISPR screening identified STAT3 or neddylation genes as positive or negative regulators of PD-L1 expression in ATLL cells.**
- **Pevonedistat improves the cytotoxic effects of the anti–PD-L1 antibody avelumab and CAR T-cells targeting PD-L1 in ATLL cells.**

Adult T-cell leukemia/lymphoma (ATLL) is an aggressive T-cell malignancy with a poor prognosis and limited treatment options. Programmed cell death ligand 1(PD-L1) is recognized to be involved in the pathobiology of ATLL. However, what molecules control PD-L1 expression and whether genetic or pharmacological intervention might modify PD-L1 expression in ATLL cells are still unknown. To comprehend the regulatory mechanisms of PD-L1 expression in ATLL cells, we performed unbiased genome-wide clustered regularly interspaced short palindromic repeat (CRISPR) screening in this work. In ATLL cells, we discovered that the neddylation-associated genes NEDD8, NAE1, UBA3, and CUL3 negatively regulated PD-L1 expression, whereas STAT3 positively did so. We verified, in line with the genetic results, that treatment with the JAK1/2 inhibitor ruxolitinib or the neddylation pathway inhibitor pevonedistat resulted in a decrease in PD-L1 expression in ATLL cells or an increase in it, respectively. It is significant that these results held true regardless of whether ATLL cells had the *PD-L1* 3′ structural variant, a known genetic anomaly that promotes PD-L1 overexpression in certain patients with primary ATLL. Pevonedistat alone showed cytotoxicity for ATLL cells, but compared with each single modality, pevonedistat improved the cytotoxic effects of the anti–PD-L1 monoclonal antibody avelumab and chimeric antigen receptor (CAR) T cells targeting PD-L1 in vitro. As a result, our work provided insight into a portion of the complex regulatory mechanisms governing PD-L1 expression in ATLL cells and demonstrated the in vitro preliminary preclinical efficacy of PD-L1–directed immunotherapies by using pevonedistat to upregulate PD-L1 in ATLL cells.

Introduction

Adult T-cell leukemia/lymphoma (ATLL) is an aggressive T-cell malignancy with a poor prognosis,[1] and therefore, there is a need to develop innovative therapeutic strategies. Previous studies have shown that ATLL has a high frequency of genetic abnormalities related to T-cell immune escape, such as loss of HLA class I expression and increased expression of programmed cell death ligand 1 (PD-L1).[2-5] This characteristic molecular pathogenesis may be related to the fact that ATLL is developed from a CD4 T cell infected with the human T-lymphotropic virus 1, which transcribes antigenic viral proteins.[6] PD-L1 plays an important role in various tumors, in which it binds PD-1 on tumor-specific CD8 T cells and attenuates the T-cell–mediated antitumor immune response. PD-L1 expression in tumor cells can be induced adaptively by tumor microenvironmental cytokines such as interferon gamma or can be driven constitutively by oncogenic signaling pathways and/or genomic aberrations in the tumor cells themselves.[7] Furthermore, it has recently been clarified that many diverse mechanisms can be involved in the regulation of PD-L1 expression, such as protein stability and subcellular localization.[8-10] A subset of ATLL cases (12%) has been reported to carry structural aberrations in the *PD-L1* 3′untranslated region (UTR), resulting in increased PD-L1 messenger RNA (mRNA) expression.[2,3] In contrast, ALK-positive anaplastic large cell lymphoma (ALK$^+$ ALCL) cases, another subtype of aggressive T-cell malignancy, have been shown to express PD-L1 with a much higher frequency (76%-100%) than ATLL, in which the disease-specific NPM-ALK chimeric protein drives PD-L1 expression by activating STAT3, MEK-ERK, and PI3K-AKT signaling pathways.[11-13] These findings suggest that some signaling

pathways might regulate PD-L1 expression in ATLL cells. However, there have been few studies on this issue. In this study, we performed unbiased genome-wide clustered regularly interspaced short palindromic repeat (CRISPR) screening[14-16] to discover genes and pathways regulating PD-L1-expression in ATLL cells. Then, we examined the mechanism-based strategies for targeting PD-L1 as therapeutic options for ATLL.

Materials and methods

See supplemental Materials and methods, available on the *Blood* website, for details.

Cell lines and cell culture

ST1, Su9T01, ATL-43Tb(−), LM-Y1(ATLL cell lines), DEL, Karpas 299, SU-DHL-1(ALK$^+$ ALCL cell lines), Jurkat, and MOLT-4 (T-cell acute lymphoblastic leukemia [T-ALL] cell lines) were maintained in RPMI 1640 supplemented with 10% fetal bovine serum (FBS) and 1% penicillin and streptomycin. KK1, KOB, and TL-Om1 were cultured in RPMI 1640 with 10% FBS, 1% penicillin and streptomycin, and 100 IU/mL human recombinant interleukin 2 (Hoffmann-La Roche, number Ro23-6019). HEK 293T was cultured in Dulbecco modified Eagle medium with 10% FBS and 1% penicillin and streptomycin. Cell lines were engineered to express human codon-optimized S. pyogenes Cas9 using the pTO-Cas9-hygro vector (Cas9 from lentiCRISPR v2 ligated into pRCMV/TO-hygro vector) or lentiCas9-Blast. LentiCRISPR v2 and lentiCas9-Blast were gifts from Feng Zhang (Addgene, plasmid numbers 52961 and 52962, respectively). The ATLL cell lines were kindly provided by the following researchers: Michiyuki Maeda (Kyoto University; ATL43Tb(−)), Yasuaki Yamada (Nagasaki University; ST1, KK1, KOB, and LM-Y1), Tomoko Hata (Nagasaki University; ST1), Naomichi Arima (Kagoshima University; Su9T01), and Kazuo Sugamura (Tohoku University; TL-Om1). ATLL cell lines were tested for unique profiles of polymorphic DNA copy number variants.[14] Expression status of HBZ and Tax in ATLL cell lines were previously confirmed.[14,15]

PBMNCs isolation and pan T cells isolation from healthy donors

Written informed consent was obtained according to the Declaration of Helsinki and approved by the Ethics Committee of the Faculty of Medicine, Hokkaido University. Peripheral blood mononuclear cells (PBMNCs) were isolated from healthy donors by Ficoll-Hypaque. Pan T cells were isolated from PBMNCs using Pan T Cell Isolation Kit, human (Miltenyi Biotec, number 130-096-535). Pan T cells and PBMNCs were cultured in RPMI 1640 with 10% FBS/1% penicillin/streptomycin/100 IU/mL human recombinant interleukin 2.

Lentivirus production and infection of sgRNA

Lentiviruses were produced using HEK 293T cells transfected with the single-guide RNA (sgRNA)-expressing lentiviral plasmids. The Cas9-expressing target cells were spin-infected with the viral supernatant with 5 μg/mL of Polybrene at 2500 revolutions per minute (rpm) at 32°C for 90 minutes.

CRISPR-Cas9 screen analysis

CRISPR-Cas9 screen was performed using Brunello CRISPR knockout pooled library containing 77 441 sgRNAs (gift of David Root and John Doench; Addgene, number 73178). Sequenced libraries were analyzed using MAGeCK software.

Production of CAR T cells

The PD-L1 chimeric antigen receptor (CAR)–expressing lentiviral plasmid was cotransfected into HEK 293T with pCAG-HIVgp (RIKEN, number RDB04394) and pCMV-VSV-G-RSV-Rev (RIKEN, number RDB04393) in a 6.9:4:4 ratio. Activated human T cells were infected with the viral supernatant concentrated via Lenti-X Concentrator (Takara, number 631232).

Immunoblot analysis

Cells were lysed in 2× sodium dodecyl sulfate sample buffer and boiled. Samples were separated on 4% to 15% Mini-PROTEAN TGX Gels (BioRad, number 4561086) and transferred to a Trans-Blot Turbo Transfer Pack (BioRad, number 1704156). Membranes were incubated with first and second antibodies, detected by enhanced chemiluminescence reagent using a ChemiDoc Touch Imaging System (BioRad).

Cell proliferation measurements

A total of 5000 to 10 000 cells per well was seeded in a final volume of 100 μL. Cell viability was measured 4 days after treatment by using Cell Counting Kit-8 (Donjindo Laboratories, number 343-07623).

Apoptosis analysis

Cells were stained with APC annexin V (BD Pharmingen, number 550474) and propidium iodide (Sigma, number P4170) and analyzed by BD FACSCantoII.

Cell cycle analysis

Cells were fixed and permeabilized with cold 70% ethanol for more than 3 hours, washed twice with FACS buffer, and resuspended with PBS, 5 μg/mL propidium iodide, and 500 μg/mL RNase A. DNA content was analyzed by BD FACSCanto II.

Statistical analysis

All experiments presented were repeated at least twice unless otherwise noted, and consistent results were obtained. Data were analyzed using Welch 2-sample *t* test by GraphPad PRISM 9. Error bars are represented as means ± standard error of the mean, unless specified otherwise; a *P* value <.05 was considered statistically significant.

Results

Unbiased genome-wide knockout CRISPR screens identify STAT3 and CMTM6 as positive regulators and neddylation-related genes as negative regulators for PD-L1 surface expression in ATLL cells

First, using flow cytometry, we examined PD-L1 cell surface expression in ATLL, ALK$^+$ ALCL, and T-ALL cell lines (Figure 1A). Mean fluorescence intensities of PD-L1 were expressed at different levels in ATLL cell lines, high levels in ALK$^+$ ALCL cell lines, and low levels in T-ALL cell lines. Therefore, we used the PD-L1 expression levels of KK1 and ST1 to undertake a genome-wide knockout CRISPR screen to find genes that upregulate and downregulate PD-L1 expression in ATLL cells,

respectively (Figure 1B). Cas9-expressing ST1 and KK1 cells were transduced with a pooled genome-wide CRISPR knockout library, selected with puromycin, and cultivated for 2 to 3 weeks, long enough for genes to be completely inactivated by sgRNAs. By using flow cytometry to determine the levels of PD-L1 surface expression, the cell populations with low levels of PD-L1 expression in ST1 and high levels of PD-L1 expression in KK1 were sorted. The numbers of each sgRNA in the sorted cells were counted by next-generation sequencing of genomic DNA and compared with the ones in the unsorted cells. The genes regulating PD-L1 expression were those for which corresponding sgRNAs were enriched in the sorted cells vs unsorted cells. We found that 9088 and 9112 genes were enriched at least $\log_2$-fold change >0 in the ST1 cells and KK1 cells, respectively, using the MAGeCK method with the 19 114 genes in the pooled library (Figure 1C; supplemental Tables 1 and 2). In the cell population expressing low levels of PD-L1 and in the population expressing high levels of PD-L1, we focused the top 10 enriched genes having 3 or 4 sgRNAs with $\log_2$-fold change >1.0 (Figure 1D). The top gene, *CD274*, which encodes the PD-L1 protein, was found among the top 10 genes whose sgRNA were enriched in the cell population expressing low levels of PD-L1. This finding validates the efficacy of our screening method. Additionally, we discovered *STAT3* and *CMTM6* in the top 10 genes. STAT3 is a known driver gene of PD-L1 expression in ALK$^+$ ALCL and extranodal natural killer/T-cell lymphoma.[11,17,18] Although it has not been reported for lymphoma cells, CMTM6 has previously been identified as the gene sustaining PD-L1 surface expression by endocytic recycling of PD-L1.[9,10] *UBA3*, *NAE1*, *NEDD8*, and *CUL3* were neddylation-related genes in the top 10 genes whose sgRNA were enriched in the cell population expressing high levels of PD-L1,[19,20] which was also validated by Gene Ontology analyses (supplemental Table 3). *PTPN2* and *SOCS3* are phosphatases associated with negative regulation of the JAK/STAT pathway, mirroring the finding of STAT3, whose sgRNA were enriched in the PD-L1 downregulated population.

STAT3 and CMTM6 promotes PD-L1 expression in ATLL cells

We created sgRNAs targeting *STAT3* and *CMTM6*, transduced KK1 cells and ST1 cells with these sgRNAs (sgSTAT3 and sgCMTM6), and then evaluated the levels of PD-L1 expression on those cells using flow cytometry (Figure 2A) to corroborate our

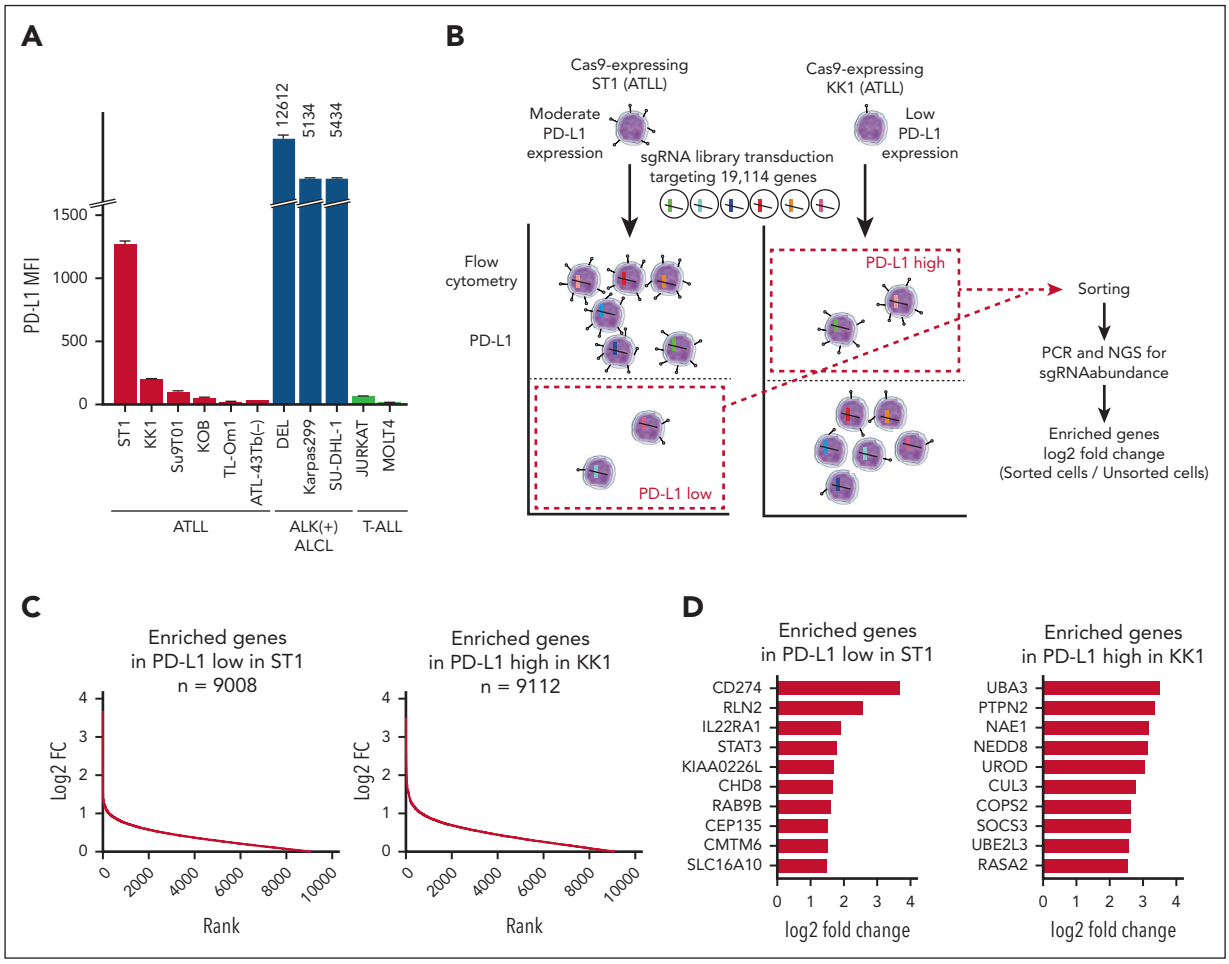

Figure 1. A CRISPR screen reveals PD-L1 regulating genes. (A) Cell surface expression of PD-L1 in ATLL cell lines, ALK$^+$ ALCL cell lines, and T-ALL cell lines measured by flow cytometry. (B) Schematic design of the CRISPR library screen in the study. Two Cas9-transducing ATLL cell lines, ST1 and KK1, were used for identifying genes whose knockout decreases or increases PD-L1 expression, respectively. (C) $\log_2$ fold-changes (sorted/unsorted population) of genes enriched in ST1 expressing low level PD-L1 (left panel) and in KK1 expressing high level PD-L1 (right panel). (D) Top 10 $\log_2$ fold change genes with 3 or 4 sgRNA $\log_2$ fold changes ≥1.0 in ST1 expressing low level PD-L1 (left panel) and in KK1 expressing high level PD-L1 (right panel).

CRISPR screen findings. As negative and positive controls, sgRNAs (sgAAVS1 and sgPD-L1) targeting AAVS1 and CD274 were also used. Cells transduced with sgPD-L1 almost lost all PD-L1 expression. STAT3 had a key role in PD-L1 expression in ATLL cells, as seen by the ~80% and 90% reduction in PD-L1 expression in ST1 and KK1 cells, respectively, in sgSTAT3-transduced cells. In ST1 and KK1 cells, sgCMTM6-transduced cells showed a 60% reduction in PD-L1 expression. Our collective screening findings for genes that support PD-L1 expression in ATLL cells were effectively verified. To see the genes associated with PD-L1 expression in primary ATLL cells, we analyzed single-cell RNA sequencing data of PBMNC from a patient with chronic-type ATLL[21] (supplemental Figure 1). In the UMAP projection, we observed PD-L1–expressing cells in ATLL cell clusters compared with the normal CD4 T-cell cluster (supplemental Figure 1A-B). When comparing gene expression between PD-L1–expressing ATLL cells vs PD-L1–null ATLL cells in the single-cell RNA sequencing data, we identified 185 differentially expressed genes (supplemental Table 4). In parallel, we identified a STAT3-regulated gene set by using the downregulated genes (> −1 in $\log_2$ fold change) in 2 sgSTAT3-transduced ATLL cell lines, ST1 and KK1, compared with the control (supplemental Table 5). Engagingly, the STAT3-regulated gene set was significantly enriched in the differentially expressed genes in PD-L1–expressing primary chronic-type ATLL cells, which was shown by gene set enrichment analysis (new supplemental Figure 1C; normalized enrichment score, 1.88; nominal $P = .011$), further supporting our screening result that STAT3 regulated PD-L1 expression in ATLL.

Given that STAT3 can be activated by multiple JAKs or receptor tyrosine kinases, we treated the ATLL lines and ALK$^+$ ALCL cells with the JAK1/2 inhibitor ruxolitinib, which is currently used for myeloproliferative neoplasms in the clinic. Surface expression of PD-L1 was strongly suppressed in KK1 and Su9T01 and modestly in ST1, indicating that JAK1/2 had a role, in part, in activating the STAT3/PD-L1 axis in ATLL cell lines (Figure 2B-C). In contrast, ALK$^+$ ALCL cells maintained PD-L1 expression under ruxolitinib treatment (Figure 2B-C), indicating ATLL and ALK$^+$ ALCL had distinct molecular mechanisms for PD-L1 expression.[11] These results indicated that PD-L1 expression could be downmodulated by using ruxolitinib through the deactivation of STAT3 in ATLL cells.

As an extended investigation, we assessed whether the ATLL cells carrying *PD-L1* 3′-UTR structural variant (SV) also depended on the JAK/STAT pathway for their PD-L1 expression. To this end, we established 2 KK1 clones having inversion of the *PD-L1* 3′-UTR region (KK1 PD-L1-SV#7 and KK1 PD-L1-SV#15-12) through CRISPR/Cas9-mediated gene editing (Figure 2D-E; supplemental Figure 2). We confirmed that these lines carrying *PD-L1* SV exhibited enhanced PD-L1 expression (Figure 2E). Importantly, ruxolitinib treatment suppressed the amount of activated form of STAT3 (phosphorylated STAT3 [pSTAT3]) as well as PD-L1 expression in both KK1 PD-L1-SV#7 and KK1 PD-L1-SV#15-12, indicating that SV-mediated PD-L1 overexpression can be therapeutically targeted (Figure 2F-G).

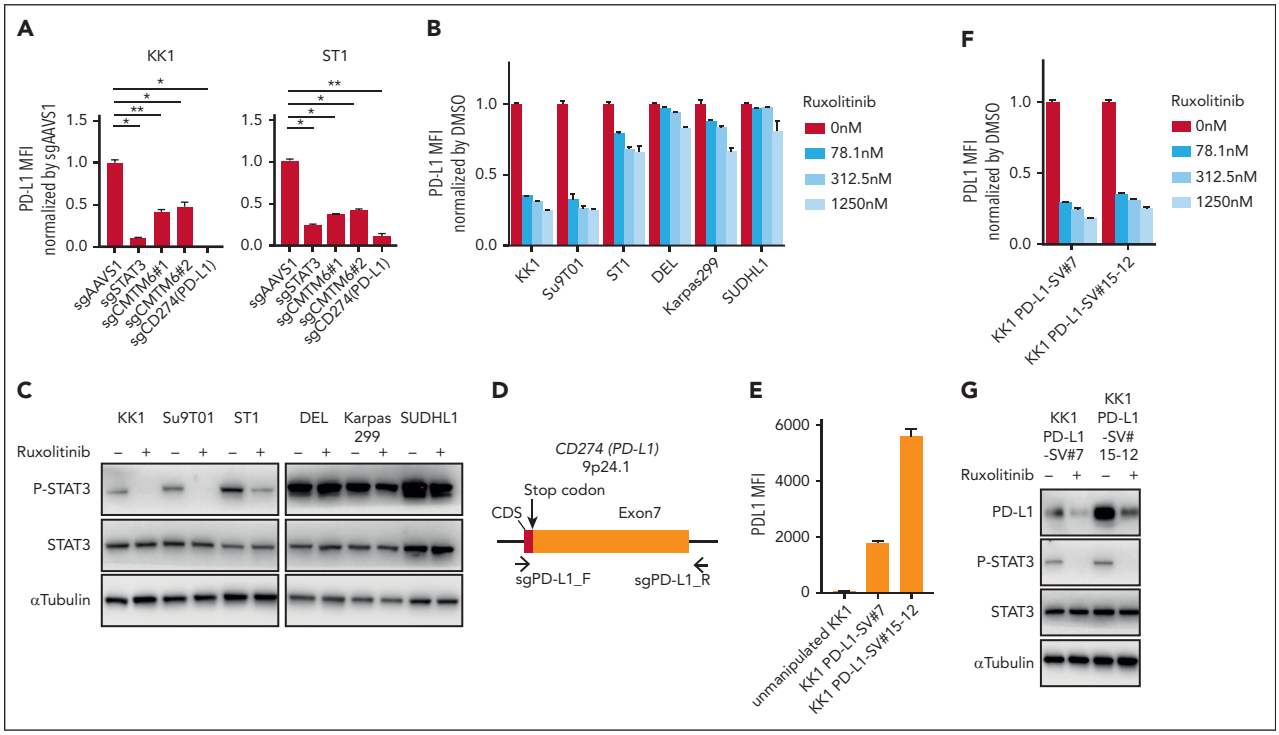

Figure 2. STAT3 inhibition suppresses PD-L1 expression in ATLL cells. (A) Cell surface expression of PD-L1 in KK1 and ST1 ATLL cells transduced with the indicated sgRNA by flow cytometry. PD-L1 mean fluorescent intensity (MFI) was normalized by that of control sgRNA (sgAAVS1)-transduced cells. (B) Cell surface expression of PD-L1 in ATLL (KK1, Su9T01, and ST1) and ALK+ ALCL (DEL, Karpas299, and SUDHL1) cells treated with ruxolitinib for 24 hours by flow cytometry. MFI was normalized by that of dimethyl sulfoxide (DMSO)-treated cells. (C) Immunoblot analysis of p-STAT3, STAT3 and α-tubulin in ruxolitinib-treated ATLL and ALK$^+$ ALCL cells. (D) Schema for the genomic locations targeted by sgRNAs for CRISPR/Cas9-mediated gene editing in the PD-L1 3′-UTR region. (E-F) Cell surface expression of PD-L1 in KK1 PD-L1 SV#7 cells and KK1 PD-L1 SV#15-12 cells by flow cytometry. The cells were treated with the indicated concentrations of ruxolitinib for 24 hours, and MFI was normalized by that of DMSO-treated cells in panel F. (G) Immunoblot analysis of PD-L1, p-STAT3, STAT3, and α-tubulin in KK1 PD-L1 SV#7 cells and KK1 PD-L1 SV#15-12 cells treated with or without ruxolitinib (312.5 nM) for 24 hours. Error bars represent the mean with standard error of the mean (SEM) of replicates. *$P < .05$; **$P < .01$, Welch 2-sample t test. All experiments were repeated at least 2 times.

The neddylation pathway suppresses PD-L1 expression in ATLL cells

We created sgRNAs (sgUBA3, sgNEDD8, sgCUL3, and sgNAE1) that specifically targeted the neddylation pathway genes *UBA3*, *NEDD8*, *CUL3*, and *NAE1*. Compared with sgAAVS1-transduced control cells, both KK1 and ST1 cells transduced with these sgRNAs displayed elevated cell surface PD-L1 expression (Figure 3A). Immunoblot analysis further supported these results (Figure 3B).

Neddylation is a protein posttranslational modification that covalently conjugates a ubiquitin-like protein NEDD8 to the substrate proteins. The NEDD8-activating enzyme (NAE), which consists of the NAE1 and UBA3 subunits, catalyzes this reaction. Cullin-RING ubiquitin ligases are activated by neddylated cullin (CUL1-7), and as a result, their protein substrates are more likely to be ubiquitylated.[19,20] In order to determine whether PD-L1 expression may be pharmacologically modulated, we treated the ATLL lines and ALK$^+$ ALCL cells with pevonedistat,[22] a NAE inhibitor. PD-L1 treatment increased PD-L1 surface expression in at least 5 ATLL cell lines (KK1, ST1, Su9T01, KOB, and TL-Om1; supplemental Figure 3A-B; Figure 4A). PD-L1 was hardly surface stained in the remaining 2 ATLL cell lines, ATL43Tb(−) and LM-Y1, at baseline (supplemental Figure 3A), but pevonedistat boosted PD-L1 expression in a dose-dependent manner (Figure 4A). The PD-L1 expression of ALK$^+$ ALCL and T-ALL cell lines was not significantly affected by pevonedistat (Figure 4A).

Next, we sought to interrogate the mechanism of PD-L1 upregulation by NAE inhibition. Treatment with pevonedistat increased PD-L1 mRNA as well as protein levels in ATLL cells (Figure 4B), indicating that transcriptional upregulation may be the root of pevonedistat-mediated PD-L1 upregulation. Given that STAT3 is required for PD-L1 production in ATLL cells (Figure 2A), we used an immunoblot to measure the concentration of pSTAT3 in ATLL cells after pevonedistat treatment. Pevonedistat activity was confirmed by CUL5, a recognized neddylation substrate, which decreased its neddylated form (Figure 4C, arrowhead at panels of CUL5). Both pSTAT3 and PD-L1 levels were significantly higher in these pevonedistat-treated cells, indicating that STAT3 activation may be the root cause of pevonedistat-mediated PD-L1 expression (Figure 4C). In fact, ruxolitinib therapy and sgSTAT3-transduction both prevented pevonedistat-mediated PD-L1 overexpression (Figure 4D-F). These findings demonstrated that pevonedistat activated STAT3 in ATLL cells, which in turn increased PD-L1 expression.

We investigated whether pevonedistat might alter the expression of PD-L1 in ATLL cells that have the *PD-L1* 3′-UTR SV. PD-L1 expression was already high in ATLL cells bearing *PD-L1* 3′-UTR SV, and pevonedistat further increased PD-L1 expression in these ATLL cells (Figure 4G). Treatment with roxolitinib prevented pevonedistat-mediated PD-L1 expression in KK1 PD-L1-SV#7 and KK1 PD-L1-SV#15-12, indicating that pevonedistat induced PD-L1 expression by activating STAT3 in ATLL cells that carried the *PD-L1* 3′-UTR SV (Figure 4H).

STAT3 gain-of-function mutations were found in 26.7% of ATLL cases, and we previously reported that ectopic expression of mutated STAT3 complementary DNA exhibited enhanced pSTAT3[15] in ATLL cells. We found that the mutated STAT3-transduced ATLL cells increased PD-L1 expression (Figure 4I), and pevonedistat treatment further augmented PD-L1 expression (Figure 4I-J).

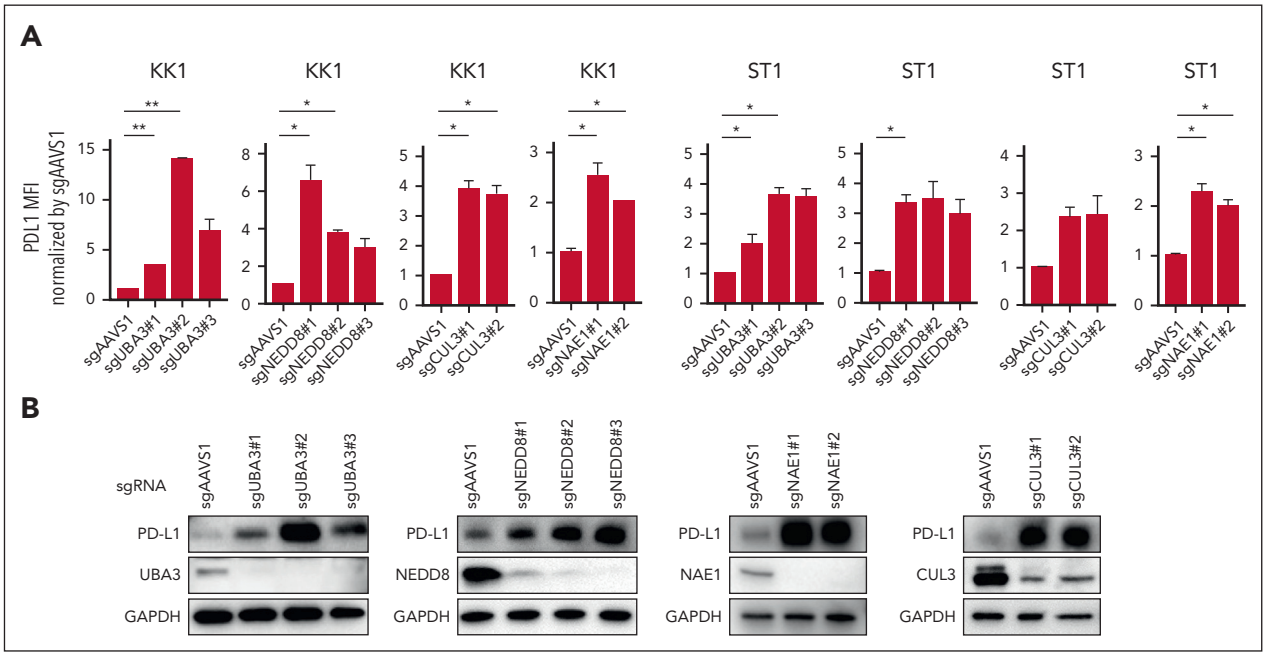

Figure 3. Neddylation inhibition increases PD-L1 expression in ATLL cells. (A) Cell surface expression of PD-L1 in KK1 and ST1 ATLL cells transduced with the indicated sgRNA by flow cytometry. (B) Immunoblot analysis of PD-L1, UBA3, NEDD8, NAE1, CUL3, and glyceraldehyde-3-phosphate dehydrogenase (GAPDH) in sgAAVS1, sgUBA3, sgNEDD8, sgNAE1, and sgCUL3-transduced KK1 cells. Error bars represent the mean with SEM of replicates. *P < .05; **P < .01; Welch 2-sample t test. All experiments were repeated at least twice.

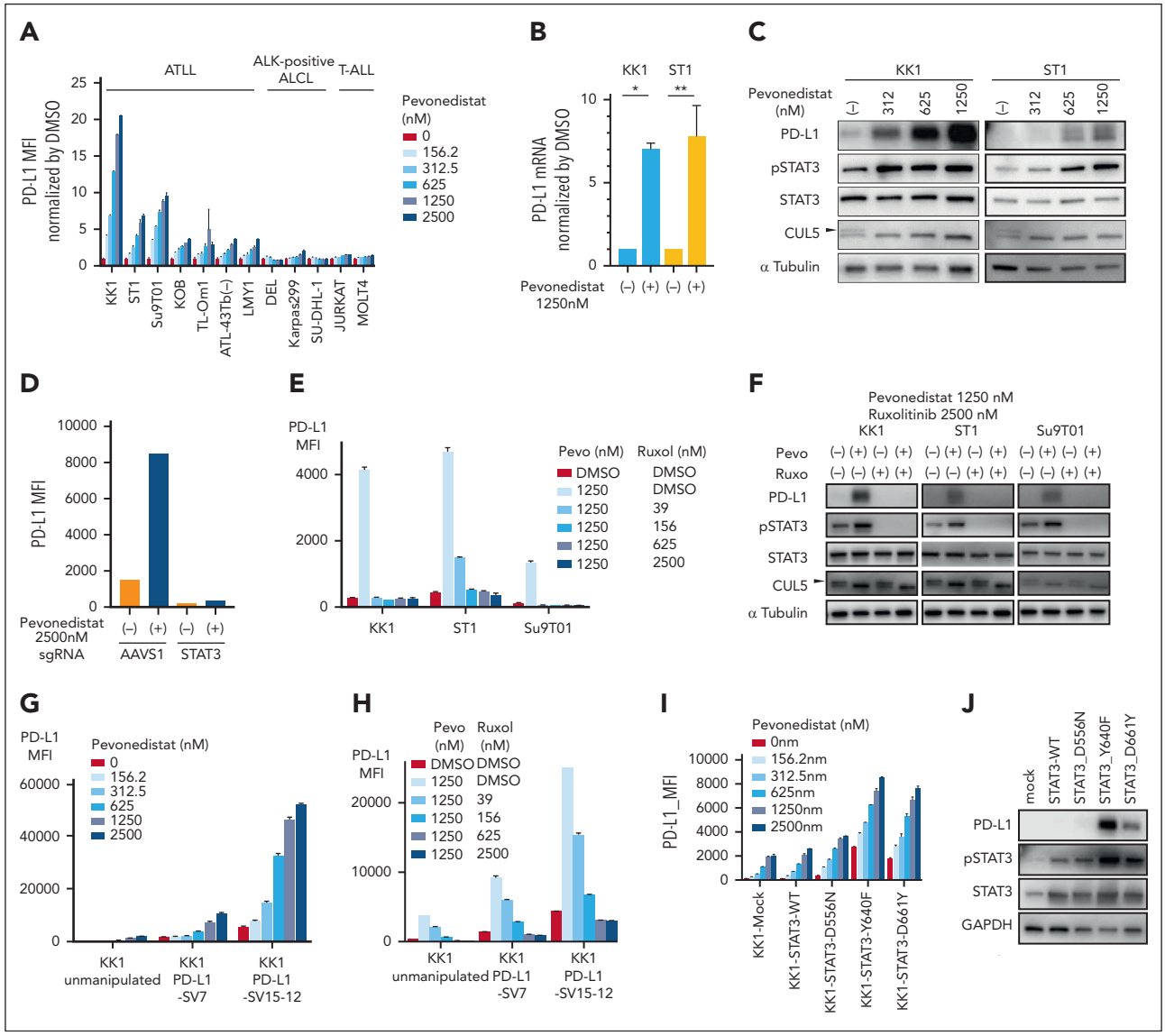

Figure 4. Pevonedistat increases PD-L1 expression in ATLL cells. (A) Cell surface expression of PD-L1 in ATLL, ALK$^+$ ALCL, and T-ALL cell lines treated with the indicated concentration of pevonedistat for 24 hours measured by flow cytometry. The y-axis represents MFI normalized by that of DMSO-treated cells. (B) mRNA expression of PD-L1 in KK1 and ST1 ATLL cells treated with pevonedistat for 24 hours as measured by the TaqMan gene expression assay. (C) Immunoblot analysis of PD-L1, pSTAT3, STAT3, CUL5, and α-tubulin in KK1 and ST1 ATLL cells treated with the indicated amount of pevonedistat for 24 hours. The arrowhead indicates the neddylated form of CUL5, which was decreased by using pevonedistat. (D) ST1 cells transduced with sgSTAT3 together with a GFP reporter or with a control sgAAVS1 were treated with pevonedistat for 24 hours. Cell surface expression of PD-L1 in the GFP-expressing cell populations was measured by flow cytometry. (E) Cell surface expression of PD-L1 in KK1, ST1, and Su9T01 ATLL cell lines treated with the indicated concentrations of pevonedistat and ruxolitinib for 24 hours was measured by flow cytometry. (F) Immunoblot analysis of PD-L1, pSTAT3, STAT3, CUL5, and α-tubulin in KK1, ST1, and Su9T01 ATLL cells treated with the indicated amounts of pevonedistat and ruxolitinib for 24 hours. The arrowhead indicates the neddylated form of CUL5. (G-H) Cell surface expression of PD-L1 in unmanipulated KK1, KK1 PD-L1 SV#7, and KK1 PD-L1 SV#15-12 cells treated with the indicated amount of pevonedistat (G) or with a combination of pevonedistat and ruxolitinib (H) for 24 hours was measured by flow cytometry. (I) Cell surface expression of PD-L1 in the mutated STAT3-transduced KK1 ATLL cells treated with the indicated amount of pevonedistat for 24 hours was measured by flow cytometry. (J) Immunoblot analysis of PD-L1, pSTAT3, STAT3, and GAPDH in the mutated STAT3-transduced KK1 ATLL cells. Error bars represent the mean with SEM of replicates. *P < .05; **P < .01; Welch 2-sample t test. All experiments were repeated at least twice. GFP, green fluorescent protein.

Pevonedistat inhibits ATLL cell line proliferation

Pevonedistat's cytotoxicity has been shown in preclinical investigations in a number of cancer models,[22,23] and a phase 1 clinical trial[24,25] in B-cell non-Hodgkin lymphoma revealed the drug's favorable safety profile. To see whether pevonedistat could inhibit ATLL cell proliferation, we treated ATLL cells with pevonedistat. With the exception of ATL-43Tb(–), all ATLL cell lines underwent a 4-day pevonedistat treatment that drastically decreased the number of viable cells (Figure 5A). In ATLL lines, pevonedistat administration significantly and time-dependently induced apoptosis (Figure 5B-C). Pevonedistat also caused cell cycle arrest in ATLL lines during the S and G2/M phases (Figure 5D). Together, apoptosis induction and cell cycle arrest caused pevonedistat to have cytotoxic effects on ATLL cells. In contrast, resting CD4 T-cell derived from 2 healthy donors were less susceptible to pevonedistat, although activated CD4 T cells were susceptible to pevonedistat at comparable level with ATLL lines (supplemental Figure 4A-F).

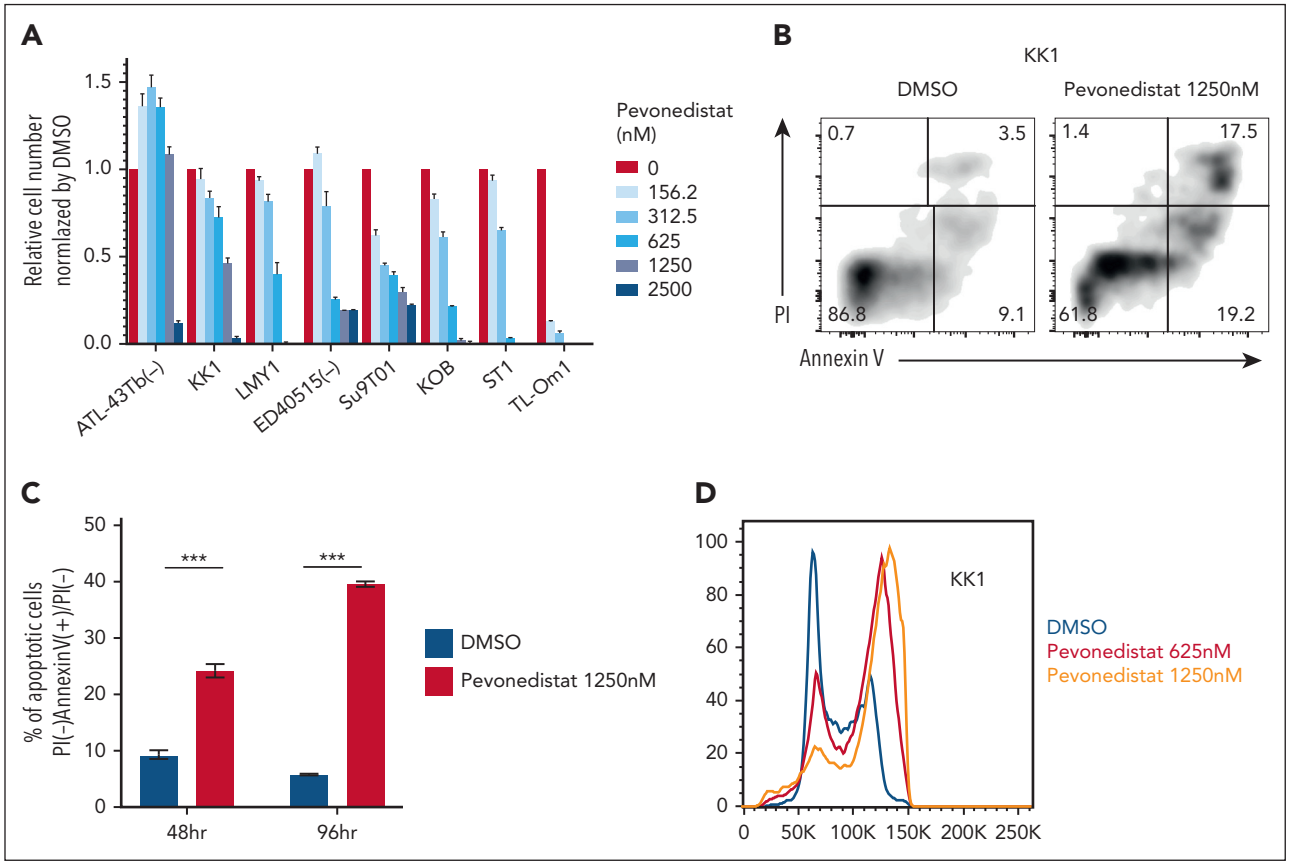

Figure 5. Pevonedistat induces apoptosis and cell cycle arrest in ATLL cell lines. (A) Viable cell numbers measured by the MTS assay for ATLL cell lines treated with the indicated amount of pevonedistat for 96 hours. (B) The percentages of apoptotic cells in KK1 cells treated with or without pevonedistat at 1250 nM for 48 hours were detected by analyzing annexin V and propidium iodide (PI) on flow cytometry. (C) The percentage of PI(–) annexin V(+)/PI(–) KK1 cells treated with or without pevonedistat at 1250 nM was monitored at 48 and 96 hours. The black and red bars represent DMSO- or pevonedistat-treated cells, respectively. (D) DNA content was analyzed in KK1 cells with or without pevonedistat for 48 hours. Error bars represent the mean with SEM of replicates. ***$P < .001$, Welch 2-sample t test. All experiments were repeated at least twice.

A combination of pevonedistat and the anti–PD-L1 monoclonal antibody avelumab effectively eradicates ATLL cells

Avelumab is a fully human immunoglobulin G1 monoclonal antibody targeting PD-L1 and has been clinically used for the treatment of patients with metastatic Merkel cell carcinoma, advanced or metastatic urothelial carcinoma, and advanced renal cell carcinoma. Avelumab has the unique capacity to exert immune checkpoint inhibition and antibody-dependent cell-mediated cytotoxicity (ADCC).[26] We hypothesized that avelumab could exert better cytotoxic efficacy in ATLL cells with enhanced PD-L1 expression than with ones without. To this end, we used STAT3^{Y640F}-transduced KK1 (KK1-STAT3^{Y640F}) and KK1 PD-L1-SV#7 as target cells for avelumab. The target cells were incubated with avelumab for 1 hour, and then the effector PBMNCs were added to the target cells (Figure 6A-B). After a 3- to 4-hour incubation, the live target cells were counted by flow cytometry. Importantly, KK1-STAT3^{Y640F} and KK1 PDL1-SV#7 were more efficiently eradicated than wild-type KK1 cells, indicating the amount of PD-L1 expression was associated with avelumab-mediated ADCC (Figure 6A-B).

We hypothesized that pevonedistat might improve the therapeutic effectiveness of avelumab because it increased PD-L1 expression and caused cytotoxicity in ATLL cells. Pevonedistat was applied to KK1 cells for 24 hours, after which the pretreated KK1 cells were cocultured with PBMNC and avelumab for 4 hours (Figure 6C). Even at a 0:1 effector:target ratio (ET ratio), we observed a drop in the number of living KK1 cells, which suggests that the pevonedistat pretreatment was cytotoxic for long term (supplemental Figure 5A). In the presence of avelumab, the specific lysis of KK1 cell was drastically increased in an ET ratio–dependent way (Figure 6C). This was the case with ST1 cells expressing higher level PD-L1 (supplemental Figure 5B) but not with TL-Om1 cells expressing lower level PD-L1 (supplemental Figure 5C), supporting the notion that the expression levels of PD-L1 were correlated to the avelumab efficacies. It is significant that these results held true for KK1 PD-L1 SV#7 cells as well (Figure 6D; supplemental Figure 5D). Our observations as a whole were consistent with the idea that pevonedistat administration improved the cytotoxic effectiveness of avelumab in ATLL cells with increased PD-L1 expression.

A combination of pevonedistat with PD-L1 CAR T cells effectively eradicates ATLL cells

CAR T-cell therapy is one of the major breakthroughs in the treatment of hematological malignancies.[27-29] Although anti-B cell maturation antigen (BCMA)/CD19 CAR T cells have been shown to be highly effective for the treatment of B-cell

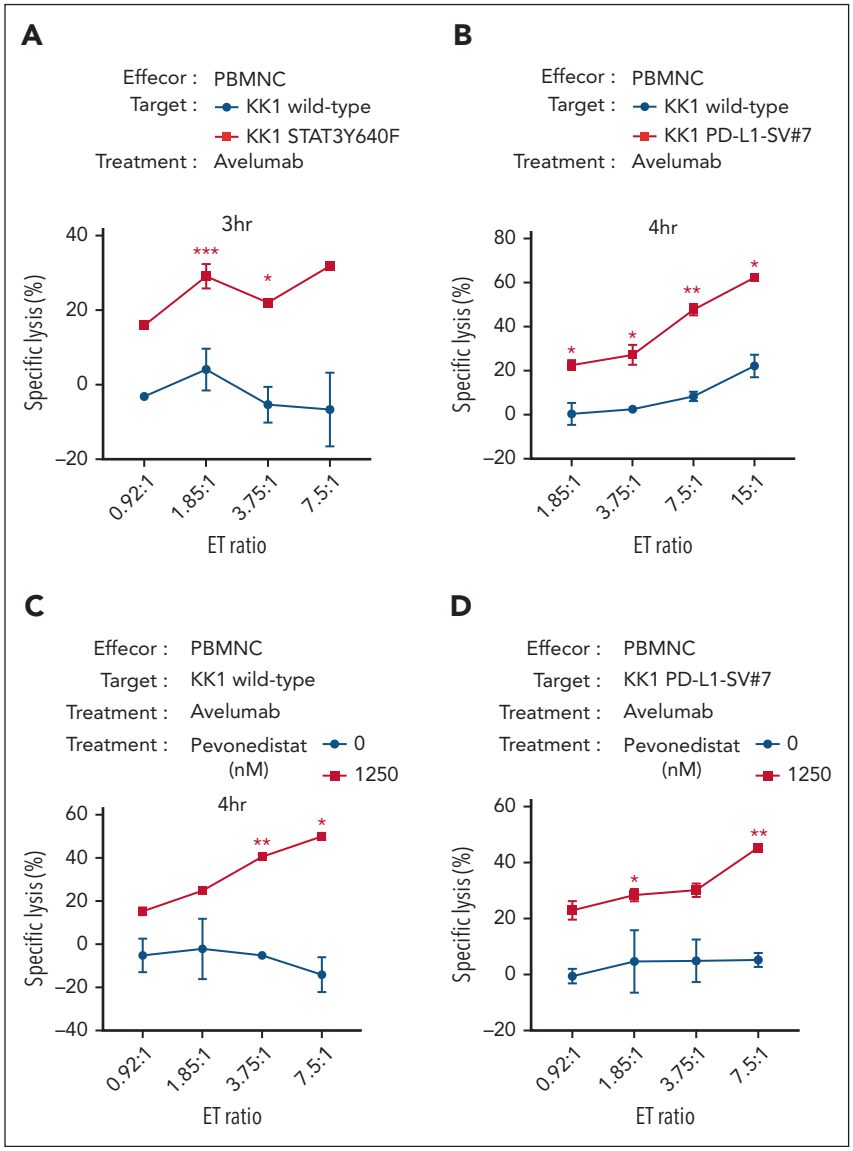

Figure 6. Pevonedistat can enhance the cytotoxicities of anti–PD-L1 monoclonal antibody avelumab in ATLL cells. (A) Values of specific lysis of the target KK1 cells with or without ectopic STAT3^{Y640F} cDNA expression under cocultivation with the effector PBMNC. The target cells were stained with CellBriteTM Red Cytoplasmic Membrane dye for the discrimination from effector cells and treated with 1 μg/mL avelumab for 1 hour before coculture. After the cocultivation of the target KK1 cells and the effector PBMNC for the indicated time, the dye-stained target cell numbers were analyzed by flow cytometry. The numbers were normalized by cell counting beads. (B) The target KK1 wild type or KK1 PD-L1-SV#7 cells were analyzed as shown in panel A. (C-D) The target KK1 wild-type cells (C) or KK1 PD-L1-SV#7 (D) were pretreated with or without pevonedistat for 24 hours. After washing, the target cells were analyzed as shown in panel A. Error bars represent the mean with SEM of replicates. *$P < .05$; **$P < .01$; ***$P < .001$; Welch 2-sample t test. All experiments were repeated at least 2 times. cDNA, complementary DNA.

malignancies, other CAR T cells have been under investigation to treat other types of malignancies. PD-L1–targeted CAR (PD-L1 CAR) T cells have been recently proposed to kill PD-L1–expressing tumor cells as well as cells in the tumor microenvironment and are likely to be an effective CAR T-cell therapy.[30,31] Given that avelumab-mediated PD-L1 targeting was enhanced by pevonedistat treatment (Figure 6D) and the activity of various CAR T cells was reported to be highly dependent on target antigen density,[32-34] we investigated whether pevonedistat could enhance the therapeutic efficacy of PD-L1 CAR T cells. To address this, we constructed a CAR complementary DNA encoding a durvalumab-based anti–PD-L1 single-chain variable fragment, CD8a hinge and transmembrane region, 4-1BB intracellular domain, and CD3z (zeta) signaling domain and inserted the construct into a bicistronic lentiviral vector expressing a Venus reporter gene (Figure 7A). CD3/CD28-stimulated T cells from healthy donors were lentivirally transduced using the PD-L1 CAR vector or mock vector. The infected cell population and the surface expression level of PD-L1 CAR were confirmed by flow cytometry using Venus reporter and phycoerythrin-conjugated L-protein staining, respectively (Figure 7B). PD-L1 CAR T cells killed KK1 ATLL cells efficiently but failed to do so for the PD-L1 knockout KK1 cells, confirming the specific killing capacity of the PD-L1 CAR T cells (Figure 7C-D). Then we asked whether ATLL cells with PD-L1 SV were more sensitive to the PD-L1 CAR T cells. We used KK1 PD-L1 SV#7 cells and KK1 PD-L1 SV#15-12 cells, expressing PD-L1 moderately and highly, respectively, as well as unmanipulated KK1 cells as target cells. PD-L1 CAR T cells killed KK1 PD-L1 SV#7 cells and KK1 PD-L1 SV#15-12 cells more efficiently than unmanipulated KK1 cells (Figure 7E). These results indicated that the amount of PD-L1 surface expression affected the killing efficiency of PD-L1 CAR T cells.

Next, we looked at whether pevonedistat therapy improved PD-L1 CAR T-cell–mediated cytotoxicity. Before the killing experiment, unmanipulated KK1 cells, KK1 PD-L1 SV#7 cells, and KK1 PD-L1 SV#15-12 cells were preincubated with

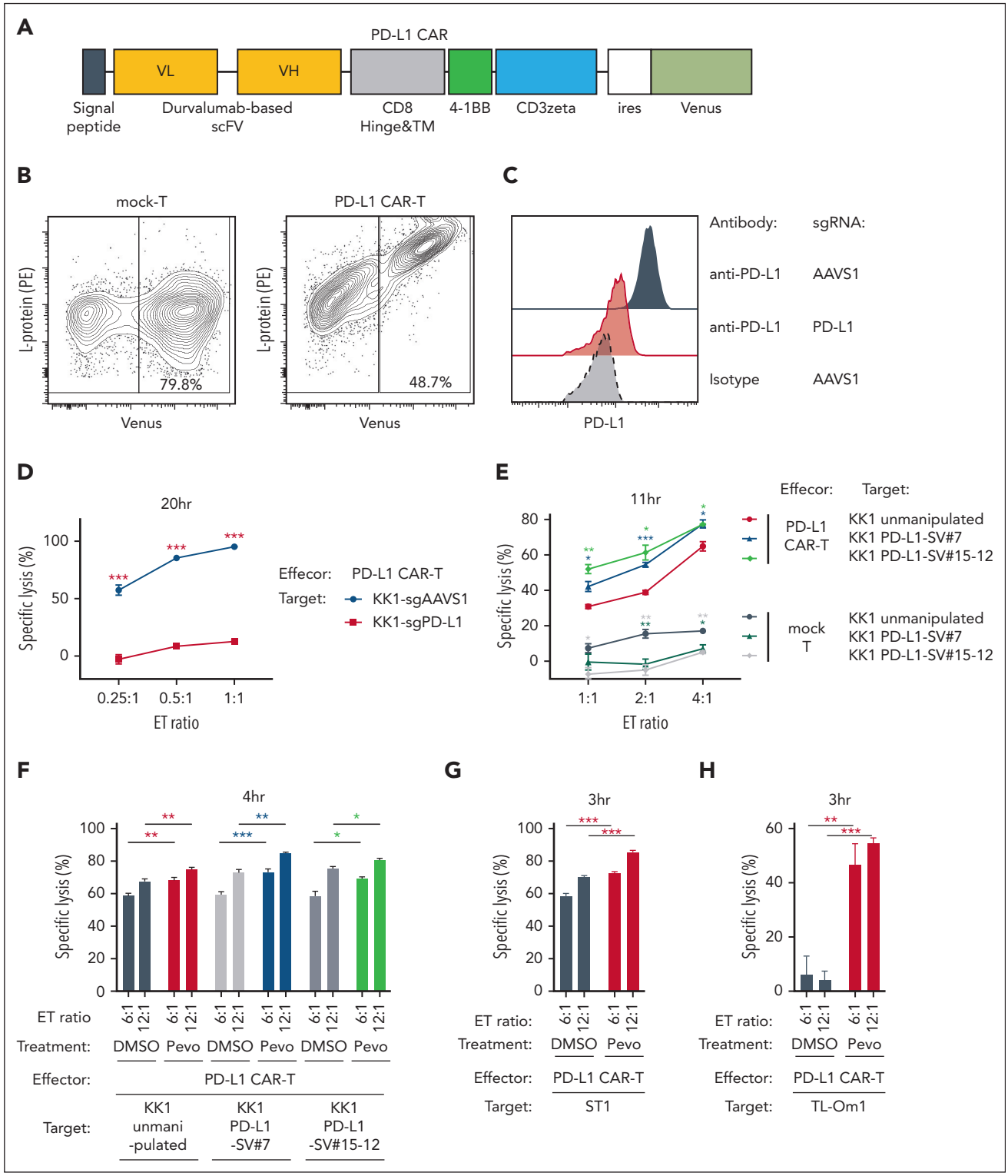

Figure 7. Pevonedistat can enhance the cytotoxicities of PD-L1 CAR T cells in ATLL cells. (A) Schematic design of the durvalumab-based anti–PD-L1 CAR construct used in the study. (B) Representative plots showing the transduction efficiency of mock-control T cells and PD-L1 CAR T cells analyzed by flow cytometry. (C) Cell surface expression of PD-L1 in KK1 cells transduced with sgAAVS1 or sgPD-L1 was measured via flow cytometry. PD-L1 knockout KK1 cells were established by single-cell cloning from bulk sgPD-L1–transduced cells. (D) Values of specific lysis of KK1 cells transduced with sgAAVS1 or sgPD-L1 under cocultivation with PD-L1 CAR T cells. Data were obtained as shown in Figure 6A. (E) Values of specific lysis of unmanipulated KK1 (wild-type), KK1 PD-L1-SV#7, and KK1 PD-L1-SV#15-12 cells under cocultivation with mock T cells and PD-L1 CAR T cells. Data were obtained as shown in Figure 6A. (F-H) Values of specific lysis of unmanipulated KK1 (wild-type) (F), KK1 PD-L1 SV#7 (F), KK1 PD-L1 SV#15-12 (F), unmanipulated ST1 (G), and unmanipulated TL-Om1 cells (H) under cocultivation with the effector PD-L1 CAR T cells. The target cells were pretreated with pevonedistat (1250 nM) or DMSO for 24 hours, washed twice, stained with CellBrite red cytoplasmic membrane dye, and cocultured with the effector PD-L1 CAR T cells. Data were obtained as shown in Figure 6A. Error bars represent the mean with SEM of replicates. *$P < .05$; **$P < .01$; ***$P < .001$; Welch 2-sample t test. All experiments were repeated at least 2 times.

pevonedistat for 24 hours. For 4 hours, control T cells or PD-L1 CAR T cells were cocultured with pretreated KK1 cells. Statistically significantly better than dimethyl sulfoxide-treated KK1 cells, PD-L1 CAR T cells killed pevonedistat-treated unmanipulated KK1 cells, KK1 PD-L1 SV#7 cells, and KK1 PD-L1 SV#15-12 cells (Figure 7F; supplemental Figure 6A). This is also the case with unmanipulated ST1 and TL-Om1 cells treated with PD-L1 CAR T cells (Figure 7G-H). These findings suggested that pevonedistat, particularly in ATLL cells bearing *PD-L1* SV, might enhance the cytotoxic effect of PD-L1–targeting CAR T cells by raising PD-L1 expression.

Discussion

We performed a genome-wide knockout CRISPR screen and identified STAT3 and neddylation-related genes as core regulatory mechanisms of PD-L1 expression in ATLL cells. The use of pevonedistat,[22] a NAE inhibitor, increased p-STAT3, which drove PD-L1 expression. Importantly ATLL cells having a 3′ UTR SV or carrying a STAT3 gain-of-function mutation also retain the core regulatory mechanism of PD-L1 expression. Specifically, KK1 PD-L1-SV#15-12 had a 100-fold increase in PD-L1 expression compared with unmanipulated KK1 cells, and pevonedistat treatment at 2500 nM enhanced a further 9.3-fold increase in PD-L1 expression, resulting in a 9300-fold increase in total. It has been reported that inactivation of NAE1 and UBA3 or pevonedistat treatment promoted PD-L1 expression in glioblastoma, lung cancer, and pancreatic cancer cells through c-MYC, ERK1/2, or JNK pathway.[35,36] In contrast, pevonedistat did so in ATLL cells through STAT3 activation. Although p-STAT3–driven PD-L1 mRNA expression seems to be a common mechanism among natural killer/T-cell lymphomas cells, ALK^+ ALCL cells, and ATLL,[11,17,18] each disease might have a distinct mechanism for STAT3 activation, as illustrated by pevonedistat and ruxolitinib, which affected P-STAT3 in ATLL cells but not in ALK^+ ALCL cells.

From our screening results, 2 directions can be considered in terms of therapeutic strategy in ATLL. The first one is to inhibit the JAK-STAT3 pathway for downregulating PD-L1 expression and reactivating antitumor effector T-cell function. Currently several JAK inhibitors, including ruxolitinib, are available in clinics. However, it should be carefully considered that JAK inhibitors potentially suppress effector T-cell function as well. Another direction is to use pevonedistat to increase PD-L1 and then use PD-L1–targeting immunotherapies, such as avelumab or PD-L1 CAR T cells. The additional advantage of pevonedistat was their cytotoxicity to ATLL cells, which canceled the proliferation/survival effects of STAT3 activation in ATLL cells. We believe that patients with ATLL carrying *PD-L1* 3′ UTR SV or STAT3 mutations may benefit from the combination of pevonedistat and PD-L1–targeting immunotherapies, compared with other ATLL cases. In this setting, patients should be carefully monitored with respect to any potential risks of pevonedistat, which may trigger disease progression by PD-L1 upregulation, although phase 1 clinical trials indicated that pevonedistat with a maximum drug concentration of 3.3 to 10.3 μM had a tolerable safety profile in multiple cancer types including T-cell lymphomas.[25] Our in vitro data indicated that pevonedistat affects the viability of activated T cells (supplemental Figure 4). Thus, the scheduling and dosing of pevonedistat treatment should be carefully evaluated in preclinical and clinical settings, otherwise the advantage of CAR T cells may be weakened. In addition, it also should be noted that pevonedistat failed to meet its primary end point in the phase 3 PANTHER trial, which evaluated pevonedistat plus azacitidine vs azacitidine alone in higher-risk myelodysplastic syndromes, chronic myelomonocytic leukemia, and low–blast count acute myeloid leukemia.[37]

Therapeutic approaches using anti–PD-1 antibodies as checkpoint inhibitors have led to rapid hyperprogression in some ATLL cases.[38,39] These observations suggested that T-cell receptor signaling might be active but kept in check by the PD-1/PD-L1 axis in such ATLL cases, and anti–PD-1 antibodies would disrupt the equilibrium state. In this context, avelumab may hold an advantage for safety in terms of ATLL treatment due to its dual role of PD-1/PD-L1 blockage and ADCC function. To the best of our knowledge, this is the first report to show the utility of avelumab as well as PD-L1 CAR T cells as the potential treatment options for patients with ATLL patients.

There were several limitations in this study. First, the direct target molecule(s) for neddylation were still unknown in terms of STAT3 activation. Second, we were not able to evaluate the efficacy of a combination of pevonedistat and PD-L1–targeting immunotherapies in vivo because KK1 cells were untransplantable even in highly immunodeficient NOG mice. It is preferable that the therapeutic and adverse effects of pevonedistat combined with PD-L1–targeting immunotherapies will be carefully evaluated in xenograft model derived patient in a preclinical study. Given the efficacy demonstrated by our in vitro data and the feasibility of a clinical trial, PD-L1 CAR T cells with pevonedistat may be a priority for consideration. These unresolved issues will be evaluated in future studies. The data presented in this study are in vitro experimental, preliminary, and preclinical; however, the insights obtained in this study pave the way for exploiting this novel strategy for ATLL disease.

Acknowledgments

The authors thank Y. Yamada, T. Hata, N. Arima, and T.A. Waldmann for cell lines and C. Yokoyama for technical assistance.

This research was supported by Japan Society for the Promotion of Science KAKENHI grant number JP21H02775, research grants from The Princess Takamatsu Cancer Research Fund and Takeda Science Foundation (M.N.), by National Institutes of Health, National Cancer Institute grants R01 CA259188 and CA251674, and a scholar award from the Leukemia & Lymphoma Society (Y.Y.).

Authorship

Contribution: M.C. designed, performed experiments, analyzed data, and wrote the manuscript; J.S. designed, performed experiments, and analyzed data; T.E. designed experiments and analyzed the data; K.S. and T.I. performed experiments; H.G. and T.T. analyzed the data; H.H. and M.M. contributed vital resources; Y.Y. assisted and supported the research; and M.N. designed, performed experiments, analyzed data, wrote the manuscript, and supervised research.

Conflict-of-interest disclosure: The authors declare no competing financial interests.

ORCID profiles: M.C., 0000-0003-2731-6091; J.S., 0000-0003-1044-1654; K.S., 0000-0001-8212-5664; H.G., 0000-0001-8361-9973; H.H., 0000-0002-1822-5692; T.T., 0000-0002-0941-271X; Y.Y., 0000-0002-9948-8696; M.N., 0000-0002-8602-6054.

Correspondence: Masao Nakagawa, Department of Hematology, Hokkaido University Faculty of Medicine, Kita 15, Nishi 7, Kita-ku, Sapporo 060-8638, Japan; email: nakagawam@med.hokudai.ac.jp.

Footnotes

Submitted 6 June 2023; accepted 14 December 2023; prepublished online on *Blood* First Edition 24 December 2023. https://doi.org/10.1182/blood.2023021423.

*M.C. and J.S. contributed equally to this study.

Original data are available upon reasonable request from the corresponding author, Masao Nakagawa (nakagawam@med.hokudai.ac.jp).

The online version of this article contains a data supplement.

There is a *Blood* Commentary on this article in this issue.

The publication costs of this article were defrayed in part by page charge payment. Therefore, and solely to indicate this fact, this article is hereby marked "advertisement" in accordance with 18 USC section 1734.

REFERENCES

1. Alaggio R, Amador C, Anagnostopoulos I, et al. The 5th edition of the World Health Organization classification of haematolymphoid tumours: lymphoid neoplasms. *Leukemia*. 2022;36(7):1720-1748.
2. Kataoka K, Shiraishi Y, Takeda Y, et al. Aberrant PD-L1 expression through 3′-UTR disruption in multiple cancers. *Nature*. 2016;534(7607):402-406.
3. Kogure Y, Kameda T, Koya J, et al. Whole-genome landscape of adult T-cell leukemia/lymphoma. *Blood*. 2022;139(7):967-982.
4. Marcais A, Lhermitte L, Artesi M, et al. Targeted deep sequencing reveals clonal and subclonal mutational signatures in adult T-cell leukemia/lymphoma and defines an unfavorable indolent subtype. *Leukemia*. 2021;35(3):764-776.
5. Kataoka K, Nagata Y, Kitanaka A, et al. Integrated molecular analysis of adult T cell leukemia/lymphoma. *Nat Genet*. 2015;47(11):1304-1315.
6. Matsuoka M, Jeang KT. Human T-cell leukaemia virus type 1 (HTLV-1) infectivity and cellular transformation. *Nat Rev Cancer*. 2007;7(4):270-280.
7. Pardoll DM. The blockade of immune checkpoints in cancer immunotherapy. *Nat Rev Cancer*. 2012;12(4):252-264.
8. Zhang J, Bu X, Wang H, et al. Cyclin D-CDK4 kinase destabilizes PD-L1 via cullin 3-SPOP to control cancer immune surveillance. *Nature*. 2018;553(7686):91-95.
9. Burr ML, Sparbier CE, Chan YC, et al. CMTM6 maintains the expression of PD-L1 and regulates anti-tumour immunity. *Nature*. 2017;549(7670):101-105.
10. Mezzadra R, Sun C, Jae LT, et al. Identification of CMTM6 and CMTM4 as PD-L1 protein regulators. *Nature*. 2017;549(7670):106-110.
11. Marzec M, Zhang Q, Goradia A, et al. Oncogenic kinase NPM/ALK induces through STAT3 expression of immunosuppressive protein CD274 (PD-L1, B7-H1). *Proc Natl Acad Sci U S A*. 2008;105(52):20852-20857.
12. Yamamoto R, Nishikori M, Tashima M, et al. B7-H1 expression is regulated by MEK/ERK signaling pathway in anaplastic large cell lymphoma and Hodgkin lymphoma. *Cancer Sci*. 2009;100(11):2093-2100.
13. Zhang JP, Song Z, Wang HB, et al. A novel model of controlling PD-L1 expression in ALK(+) anaplastic large cell lymphoma revealed by CRISPR screening. *Blood*. 2019;134(2):171-185.
14. Nakagawa M, Shaffer AL 3rd, Ceribelli M, et al. Targeting the HTLV-I-regulated BATF3/IRF4 transcriptional network in adult T cell leukemia/lymphoma. *Cancer Cell*. 2018;34(2):286-297.e10.
15. Ishio T, Kumar S, Shimono J, et al. Genome-wide CRISPR screen identifies CDK6 as a therapeutic target in adult T-cell leukemia/lymphoma. *Blood*. 2022;139(10):1541-1556.
16. Chiba M, Shimono J, Ishio T, et al. Genome-wide CRISPR screens identify CD48 defining susceptibility to NK cytotoxicity in peripheral T-cell lymphomas. *Blood*. 2022;140(18):1951-1963.
17. Atsaves V, Tsesmetzis N, Chioureas D, et al. PD-L1 is commonly expressed and transcriptionally regulated by STAT3 and MYC in ALK-negative anaplastic large-cell lymphoma. *Leukemia*. 2017;31(7):1633-1637.
18. Song TL, Nairismagi ML, Laurensia Y, et al. Oncogenic activation of the STAT3 pathway drives PD-L1 expression in natural killer/T-cell lymphoma. *Blood*. 2018;132(11):1146-1158.
19. Watson IR, Irwin MS, Ohh M. NEDD8 pathways in cancer, Sine Quibus Non. *Cancer Cell*. 2011;19(2):168-176.
20. Enchev RI, Schulman BA, Peter M. Protein neddylation: beyond cullin-RING ligases. *Nat Rev Mol Cell Biol*. 2015;16(1):30-44.
21. Tan BJ, Sugata K, Reda O, et al. HTLV-1 infection promotes excessive T cell activation and transformation into adult T cell leukemia/lymphoma. *J Clin Invest*. 2021;131(24):e150472.
22. Soucy TA, Smith PG, Milhollen MA, et al. An inhibitor of NEDD8-activating enzyme as a new approach to treat cancer. *Nature*. 2009;458(7239):732-736.
23. Czuczman NM, Barth MJ, Gu J, et al. Pevonedistat, a NEDD8-activating enzyme inhibitor, is active in mantle cell lymphoma and enhances rituximab activity in vivo. *Blood*. 2016;127(9):1128-1137.
24. Torka P, Kambhampati S, Chen L, et al. Pevonedistat, a Nedd8-activating enzyme inhibitor, in combination with ibrutinib in patients with relapsed/refractory B-cell non-Hodgkin lymphoma. *Blood Cancer J*. 2023;13(1):9.
25. Shah JJ, Jakubowiak AJ, O'Connor OA, et al. Phase I study of the novel investigational NEDD8-activating enzyme inhibitor pevonedistat (MLN4924) in patients with relapsed/refractory multiple myeloma or lymphoma. *Clin Cancer Res*. 2016;22(1):34-43.
26. Boyerinas B, Jochems C, Fantini M, et al. Antibody-dependent cellular cytotoxicity activity of a novel anti-PD-L1 antibody avelumab (MSB0010718C) on human tumor cells. *Cancer Immunol Res*. 2015;3(10):1148-1157.
27. Grupp SA, Kalos M, Barrett D, et al. Chimeric antigen receptor-modified T cells for acute lymphoid leukemia. *N Engl J Med*. 2013;368(16):1509-1518.
28. Park JH, Rivière I, Gonen M, et al. Long-term follow-up of CD19 CAR therapy in acute lymphoblastic leukemia. *N Engl J Med*. 2018;378(5):449-459.
29. Jacobson CA. CD19 chimeric antigen receptor therapy for refractory aggressive B-cell lymphoma. *J Clin Oncol*. 2019;37(4):328-335.
30. Bajor M, Graczyk-Jarzynka A, Marhelava K, et al. PD-L1 CAR effector cells induce self-amplifying cytotoxic effects against target cells. *J Immunother Cancer*. 2022;10(1):e002500.
31. Liu M, Wang X, Li W, et al. Targeting PD-L1 in non-small cell lung cancer using CAR T cells. *Oncogenesis*. 2020;9(8):72.
32. Majzner RG, Rietberg SP, Sotillo E, et al. Tuning the antigen density requirement for CAR T-cell activity. *Cancer Discov*. 2020;10(5):702-723.
33. Spiegel JY, Patel S, Muffly L, et al. CAR T cells with dual targeting of CD19 and CD22 in adult patients with recurrent or refractory B cell malignancies: a phase 1 trial. *Nat Med*. 2021;27(8):1419-1431.
34. Watanabe K, Terakura S, Martens AC, et al. Target antigen density governs the efficacy of anti-CD20-CD28-CD3 zeta chimeric antigen receptor-modified effector CD8+ T cells. *J Immunol*. 2015;194(3):911-920.

35. Zhang S, You X, Xu T, et al. PD-L1 induction via the MEK-JNK-AP1 axis by a neddylation inhibitor promotes cancer-associated immunosuppression. *Cell Death Dis*. 2022; 13(10):844.

36. Zhou S, Zhao X, Yang Z, et al. Neddylation inhibition upregulates PD-L1 expression and enhances the efficacy of immune checkpoint blockade in glioblastoma. *Int J Cancer*. 2019;145(3): 763-774.

37. Ades L, Girshova L, Doronin VA, et al. Pevonedistat plus azacitidine vs azacitidine alone in higher-risk MDS/chronic myelomonocytic leukemia or low-blast-percentage AML. *Blood Adv*. 2022;6(17): 5132-5145.

38. Misawa K, Yasuda H, Matsuda H, et al. Development of acute adult T-cell leukemia following PD-1 blockade therapy for lung cancer. *Intern Med*. 2022;61(22): 3421-3424.

39. Ratner L, Waldmann TA, Janakiram M, Brammer JE. Rapid progression of adult T-cell leukemia-lymphoma after PD-1 inhibitor therapy. *N Engl J Med*. 2018; 378(20):1947-1948.